Rescue of biosynthesis of nicotinamide adenine dinucleotide protects the heart in cardiomyopathy caused by lamin A/C gene mutation

Nicolas Vignier, Maria Chatzifrangkeskou, Blanca Morales Rodriguez, Mathias Mericskay, Nathalie Mougenot, Karim Wahbi, Antoine Muchir, Gisele Bonne

HAL Id: hal-01958003

https://hal.sorbonne-universite.fr/hal-01958003v1

Submitted on 14 Jan 2019

Rescue of biosynthesis of nicotinamide adenine dinucleotide protects the heart in cardiomyopathy caused by lamin A/C gene mutation

Nicolas Vignier[1], Maria Chatzifrangkeskou[1], Blanca Morales Rodriguez[1], Mathias Mericskay[2], Nathalie Mougenot[3], Karim Wahbi[4], Gisèle Bonne[1] and Antoine Muchir[1],[*]

[1]Sorbonne Université, UPMC Paris 06, INSERM UMRS974, Center of Research in Myology, Institut de Myologie, F-75013, Paris, France, [2]INSERM UMR-S 1180 – LabEx LERMIT – DHU TORINO, Institut Paris-Saclay d'Innovation Therapeutique (IPSIT-US31-UMS3679), Faculty of Pharmacy, Univ Paris-Sud, Université Paris-Saclay, F-92296 Chatenay-Malabry, France, [3]Sorbonne Université, UPMC Paris 06, INSERM UMS28 Phénotypage du petit animal, Faculté de Médecine Pierre et Marie Curie, F-75013, Paris, France and [4]Cardiology Department, Cochin Hospital, Filière Neuromusculaire, Paris-Descartes University, Sorbonne Paris Cité University, Assistance Publique-Hôpitaux de Paris, 75014, Paris, France

[*]To whom correspondence should be addressed at: Center of Research in Myology, Sorbonne Université, UPMC-Inserm UMRS 974, Institut de Myologie G.H. Pitié Salpêtrière 47, Boulevard de l'Hopital F-75 651 Paris Cedex 13 - France. Tel: +33 142165705; Fax: +33 142165700; Email: a.muchir@institut-myologie.org

Abstract

Cardiomyopathy caused by lamin A/C gene (*LMNA*) mutations (hereafter referred as *LMNA* cardiomyopathy) is an anatomic and pathologic condition associated with muscle and electrical dysfunction of the heart, often leading to heart failure-related disability. There is currently no specific therapy available for patients that target the molecular pathophysiology of *LMNA* cardiomyopathy. Recent studies suggested that nicotinamide adenine dinucleotide (NAD^+) cellular content could be a critical determinant for heart function. Biosynthesis of NAD^+ from vitamin B3 (known as salvage pathways) is the primary source of NAD^+. We showed here that NAD^+ salvage pathway was altered in the heart of mouse and human carrying *LMNA* mutation, leading to an alteration of one of NAD^+ co-substrate enzymes, PARP-1. Oral administration of nicotinamide riboside, a natural NAD^+ precursor and a pyridine-nucleoside form of vitamin B3, leads to a marked improvement of the NAD^+ cellular content, an increase of PARylation of cardiac proteins and an improvement of left ventricular structure and function in a model of *LMNA* cardiomyopathy. Collectively, our results provide mechanistic and therapeutic insights into dilated cardiomyopathy caused by *LMNA* mutations.

Introduction

Nicotinamide adenine dinucleotide (NAD) is a metabolic co-factor found in cells either in its oxidized (NAD^+) or reduced (NADH) form. NAD^+ can be synthesized from various precursors. Biosynthesis from nicotinic acid or nicotinamide (NAM)—both present in our diet as vitamin B3—is the primary source of NAD^+ [1–3]. This pathway, also known as the salvage, is important for NAD^+ homeostasis. There is another NAD^+ precursor—nicotinamide riboside (NR)—that enhances NAD^+ levels through the salvage pathway when catalyzed by nicotinamide riboside kinase (Nmrk) [4,5]. In mammals there are two Nmrk enzymes, Nmrk1 and Nmrk2, the latter being highly restricted to muscle. In the salvage pathway of NAD^+ biosynthesis, nicotinamide phosphoribosyltransferase (Nampt) was identified as a rate-limiting enzyme that converts NAM to nicotinamide mononucleotide (NMN) [6]. NAD^+ is then synthesized from NMN by NMN adenylyltransferase (Nmnat) [7].

Studies have indicated that NAD^+ content is a critical determinant for heart function and structure [8,9] and that Nampt may play an important role in the development of dilated cardiomyopathy (DCM) [10]. In models of DCM, modulation of the different actors of the NAD salvage improves cardiac function [11–13]. DCM is characterized by dilatation and systolic dysfunction of the left or both ventricles [14]. The ventricular walls become thin and stretched, compromising cardiac contractility and resulting in altered left ventricular function. Despite current strategies to aggressively manage DCM, the disorder remains a common cause of heart failure and a prevalent diagnosis in individuals referred for cardiac transplantation. Mutations in *LMNA* encoding nuclear lamin A/C [15] were reported to cause DCM (hereafter referred to *LMNA* cardiomyopathy) [16,17]. Despite our gaps in understanding many of their fundamental functions, much of the current research on the lamin A/C is focused on how mutations within these proteins cause DCM. We asked here whether NAD^+ salvage pathway is altered and could play a role in the development of *LMNA* cardiomyopathy.

Results

Alteration of NAD^+ salvage pathway in *LMNA* cardiomyopathy

To explore the role of NAD^+ salvage pathway in the development of DCM, we studied a mouse model that displays an *Lmna* mutation changing the histidine in position 222 into a proline [18]. The male mice develop a progressive contractile dysfunction (Supplementary Material, Table 1), cardiac remodeling and die by 32–34 weeks of age [18]. *Lmna* p.H222P corresponds to a human disease-causing mutation associated with DCM [19]. Given that a consequence of altered NAD^+ salvage pathways would lead to an aberrant cellular NAD^+ content (Fig. 1A), we first assessed the steady-state cardiac NAD^+ level in both male wild-type (WT) and *Lmna*[H222P/H222P] mice. We showed that the NAD^+ content was significantly lowered in hearts from *Lmna*[H222P/H222P] mice compared with WT mice, when the left ventricular function was altered at 26 weeks (symptomatic) (Fig. 1B and C). There was a correlation between altered cardiac function and cardiac NAD^+ content, as there was no detectable decreased NAD^+ level in the heart of *Lmna*[H222P/H222P] mice at 14 weeks (pre-symptomatic) (Fig. 1B and C; Supplementary Material, Table 1).

We next assessed the expression level of enzymes from the salvage pathway of NAD^+ biosynthesis by real-time Polymerase Chain Reaction (PCR) using RNA extracted from *Lmna*[H222P/H222P] mouse hearts at 14 and 26 weeks of age. There was a significant decreased *Nampt* mRNA expression and a significant increased *Nmrk2* mRNA expression in the hearts of *Lmna*[H222P/H222P] mice compared with WT mice (Fig. 1D). In addition, *Nmnat1* mRNA expression (the nucleus isoform) was decreased at 14 weeks of age, and both cardiac mRNA expression levels of *Nmnat1* and *Nmnat3* (the mitochondrial isoform) were significantly decreased in *Lmna*[H222P/H222P] mice at 26 weeks of age, compared with WT mice (Fig. 1D). We then evaluated the expression of Nampt, Nmrk2 and Nmnat1 at the protein level. The deregulation of the protein expression level was in concordance with mRNA expression level in hearts from *Lmna*[H222P/H222P] mice compared with WT mice at 26 weeks of age (Fig. 1E). While these results strongly suggest that abnormal NAD^+ salvage pathway contributes to the development of cardiomyopathy in *Lmna*[H222P/H222P] mice, its pathogenic role in affected skeletal muscles is unknown. Based on our findings in heart, we hypothesize that abnormal NAD^+ salvage pathway is similarly involved in the pathogenesis of skeletal muscular dystrophy in the *Lmna*[H222P/H222P] mouse model. Furthermore, we showed a significant drop of NAD^+ content (Fig. S1A), a significant decreased *Nampt* and *Nmnat1* and increased *Nmrk2* mRNAs expression (Fig. S1B) in soleus from *Lmna*[H222P/H222P] mice at 26 weeks of age, compared with WT mice. We showed a similar decreased *Nampt* mRNA expression and increased *Nmrk2* mRNA expression in the hearts of another mouse model of *LMNA* cardiomyopathy, *Lmna*[delK32/+] mice [20], at 26 weeks of age compared with WT mice, when the left ventricular function was severely altered (Fig. S2A and S2B). The same expression pattern of these key genes was also found in other mouse models of inherited DCM (GEO accession number: GSE54838 and GSE17478) (Fig. S1C) [21,22]. We obtained samples of heart tissue from two human subjects with *LMNA* cardiomyopathy obtained after cardiac transplantation. Control heart samples were obtained from age-matched human subjects without *LMNA* mutation. We showed decreased expression of Nampt and increased expression of Nmrk2, in heart tissue of the patients with *LMNA* mutations compared with control subjects (Fig. 1F). Taken together these results showed that the metabolism of NAD^+ is altered in *LMNA* cardiomyopathy.

Rescue of cardiac NAD^+ content by NR improves cardiac function

Given that the expression of Nmrk2 was increased in heart from *Lmna*[H222P/H222P] mice, we tested whether NR, the substrate for Nmrk2 [23], could increase NAD^+ content in the heart and therefore, blunt the development of left ventricular dysfunction. *Lmna*[H222P/H222P] mice were fed with NR-supplemented diet (400 mg/kg/day), starting at 17 weeks of age for 9 weeks duration (Fig. 2A). We first determined the NAD^+ content of NR-fed *Lmna*[H222P/H222P] mice compared with chow diet-fed *Lmna*[H222P/H222P] mice. We similarly treated WT mice and assessed the NAD^+ content. *Lmna*[H222P/H222P] mice fed with NR showed an increase of their NAD^+ content in both liver and heart (Fig. 2B). Feeding WT mice with the same concentration of NR leads similarly to increased NAD^+ content in both tissues (Fig. 2B). While around 25% of chow diet-fed *Lmna*[H222P/H222P] mice died during the duration of the protocol, we did not observed any death in the group of *Lmna*[H222P/H222P] mice fed with NR (data not shown). No significant difference in mortality was observed between NR-fed and chow diet-fed WT mice (data not shown). After NR treatment, heart size and left ventricular dilatation were reduced in *Lmna*[H222P/H222P] mice compared with chow diet-fed *Lmna*[H222P/H222P] mice (Fig. 2C). Cardiac structure and function
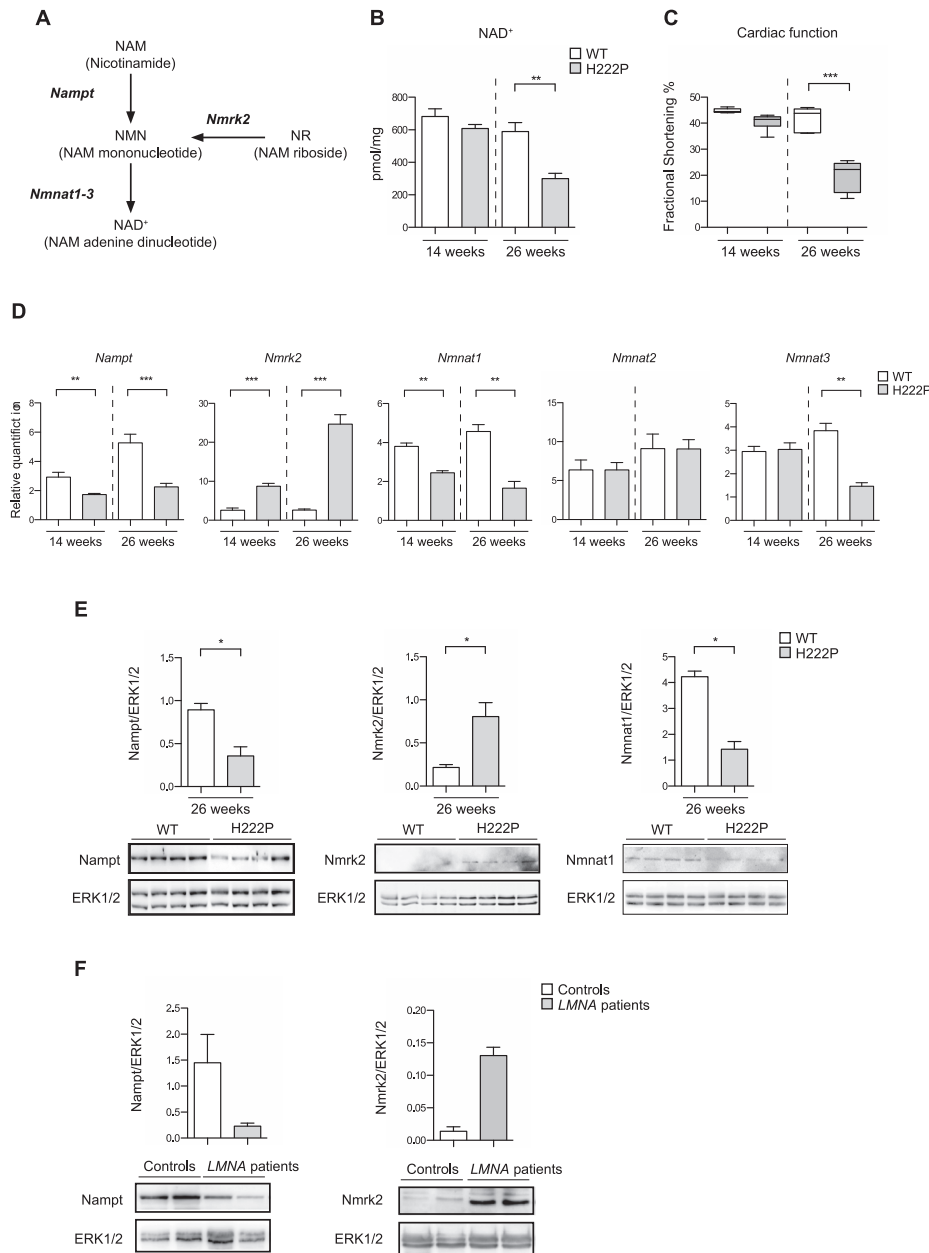
Figure 1. NAD+ salvage pathway is altered in *LMNA* cardiomyopathy **(A)** Schematic representation of the NAD+ salvage pathway. **(B)** Quantification of cardiac NAD+ content (pmol/mg tissue) in WT (n = 6) and *Lmna*^H222P/H222P^ (n = 9) mice at 14 weeks and in WT (n = 6) and *Lmna*^H222P/H222P^ (n = 7) mice at 26 weeks. Bars indicate mean ± standard error of mean. **P-value ≤ 0.001. **(C)** Box-and-whisker plots showing median fractional shortening (FS) in 14-weeks old and 26-weeks old WT and *Lmna*^H222P/H222P^ mice. Values are shown as 25th to 75th percentiles of the ranked set of data values. The line in the middle is plotted as the median. Whiskers (Tukey method) extend down to the minimum value and up to the maximum value. ***P-value ≤ 0.0001.**(D)** Expression of *Nampt, Nmrk2, Nmnat1, Nmnat2 and Nmnat3* mRNAs obtained by qPCR from WT (n = 5) and *Lmna*^H222P/H222P^ (n = 5) mice at 14 weeks and from WT (n = 5) and *Lmna*^H222P/H222P^ (n = 5) mice at 26 weeks of age. *P-value ≤ 0.01, **P-value ≤ 0.001 and ***P-value ≤ 0.0001. **(E)** Immunoblots showing Nampt, Nmrk2 and Nmnat1 protein levels in hearts from 26-weeks-old WT (n = 4) and *Lmna*^H222P/H222P^ (n = 4) mice. Representative of three independent experiments each performed in triplicates. The bar graphs represent protein relative expression (mean ± standard error of means) of Nampt and Nmrk2 (relative to ERK1/2). *P-value ≤ 0.01. **(F)** Immunoblots showing Nampt and Nmrk2 protein levels in hearts from controls (n = 2) and *LMNA* patients (n = 2). The bar graphs represent protein relative expression (mean ± standard error of mean) of Nampt (relative to ERK1/2).

were assessed by echocardiography after 4 weeks of treatment and at the end of the treatment in the four different groups of mice. Compared with chow diet-fed *Lmna*^H222P/H222P^ mice, NR-fed *Lmna*^H222P/H222P^ mice had significantly decreased left ventricular end-systolic and left ventricular end-diastolic diameters (Table 1). NR-fed *Lmna*^H222P/H222P^ mice also have improved cardiac contractility, indicated by increased left ventricular fractional shortening, starting as early as 4 weeks of treatment

(Fig. 2D, Table 1). Hence, feeding with NR for 9 weeks delayed the development of left ventricular dilatation and cardiac contractile dysfunction in *Lmna*^H222P/H222P^ mice. Compared with WT mice, *Lmna*^H222P/H222P^ mice had significantly increased expression of *Myh7*, which encodes myosin heavy chain, *Nppa*, which encodes the atrial natriuretic peptide type A and *Col1a2*, which encodes collagen (Fig. 2E). Feeding *Lmna*^H222P/H222P^ mice with NR led to a significant lowering of the expression of these markers
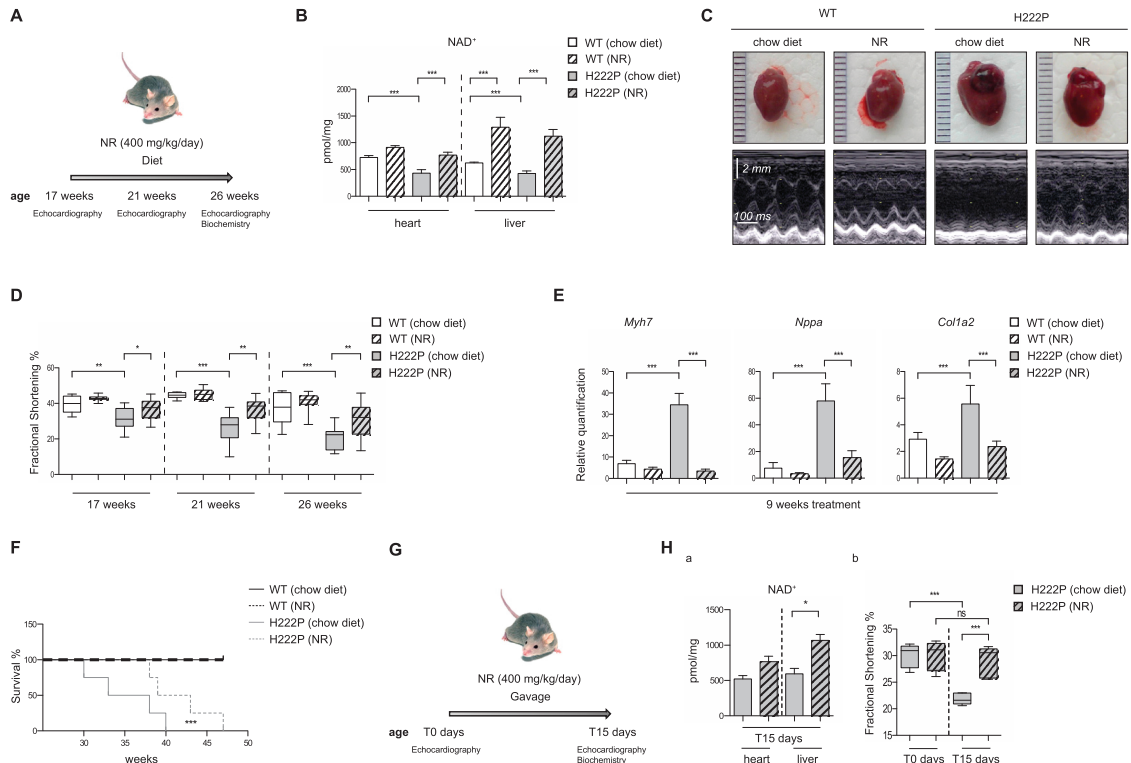
Figure 2. NR supplementation leads to cardiac improvement in $Lmna^{H222P/H222P}$ mice. (**A**) Schematic representation of the treatment protocol of WT and $Lmna^{H222P/H222P}$ mice with NR. (**B**) Quantification of NAD$^+$ content (pmol/mg tissue) in heart and liver from chow diet-fed WT (n = 7) and $Lmna^{H222P/H222P}$ (n = 8) mice and in NR fed WT (n = 7) and $Lmna^{H222P/H222P}$ (n = 26) mice at 26 weeks. Bars indicate means ± standard errors of means. ***P-value ≤ 0.0001. (**C**) Gross histological examination of heart from chow diet-fed or NR-fed WT and $Lmna^{H222P/H222P}$ mice at 26 weeks of age. (**D**) Box-and-whisker plots showing median fractional shortening (FS) in 17-, 21- and 26-weeks-old chow diet-fed or NR-fed WT and $Lmna^{H222P/H222P}$ mice. Values are shown as 25th to 75th percentiles of the ranked set of data values. The line in the middle is plotted as the median. Whiskers (Tukey method) extend down to the minimum value and up to the maximum value. *P-value ≤ 0.01, **P-value ≤ 0.001, ***P-value ≤ 0.0001. (**E**) Expression of *Myh7*, *Nppa* and *Col1a2* genes by qPCR from cDNAs of heart from chow diet-fed or NR-fed WT (n = 5) and $Lmna^{H222P/H222P}$ (n = 5) mice. ***P-value ≤ 0.0001. (**F**) Kaplan–Meier survival curves for chow diet-fed WT (n = 5) and $Lmna^{H222P/H222P}$ (n = 9) mice in NR-fed WT (n = 5) and $Lmna^{H222P/H222P}$ (n = 4) mice. ***P-value ≤ 0.0001. (**G**) Schematic representation of the treatment protocol of post symptomatic $Lmna^{H222P/H222P}$ mice with NR. (**H.a**) Quantification of NAD$^+$ content (pmol/mg tissue) in heart and liver from placebo-treated $Lmna^{H222P/H222P}$ (n = 5) mice and NR-treated $Lmna^{H222P/H222P}$ (n = 5) mice at 26 weeks. Bars indicate means ± standard errors of means. *P-value ≤ 0.01. (**H.b**) Box-and-whisker plots showing median fractional shortening (FS) in 17-, 21- and 26-weeks-old placebo-treated or NR-treated $Lmna^{H222P/H222P}$ mice. Values are shown as 25th to 75th percentiles of the ranked set of data values. The line in the middle is plotted as the median. Whiskers (Tukey method) extend down to the minimum value and up to the maximum value. ***P-value ≤ 0.0001, NS: non significant.

of cardiac remodeling compared with chow diet-fed animals (Fig. 2E). NR-fed $Lmna^{H222P/H222P}$ mice exhibited a decreased mRNA expression of *Nmrk2* but *Nampt* mRNA expression was unchanged, compared with chow diet-fed $Lmna^{H222P/H222P}$ (Fig. S3A). In a pilot study, we assessed the effect of NR treatment on survival. The mean survival was significantly prolonged in NR-fed $Lmna^{H222P/H222P}$ mice compared with chow diet-fed mice (Fig. 2F). Taken together, these results showed that NR supplemented diet is efficient to partially restore the left ventricular function and increase the survival in a mouse model of LMNA cardiomyopathy.

A critical question relevant to potential treatment of patients with NR regards their effectiveness after the onset of cardiac dysfunction. To help answer this question, we assessed the benefit of NR after dilatation and decreased cardiac fractional shortening have already occurred. $Lmna^{H222P/H222P}$ mice were treated with NR (daily oral dose, 400 mg/kg per day), starting when left ventricular fractional shortening was significantly lowered (30%) compared with WT mice. NR increased NAD$^+$ content in both liver and heart compared with placebo (Fig. 2H.a). We used M-mode echocardiograph to image *in vivo* and assess left ventricular diameters. It showed that left ventricular dimensions and fractional shortening remained stable during the course of the treatment in $Lmna^{H222P/H222P}$ mice while this parameters were decreased in placebo-treated mice (Fig. 2H.b; Supplementary Material, Table S2)

Nicotinamide supplement is not beneficial for the cardiac function in LMNA cardiomyopathy

We next assessed the benefit of NAM (the substrate for Nampt) on the left ventricular function. If our hypothesis posits that NAD$^+$ salvage signaling plays a role in the pathogenesis of LMNA cardiomyopathy, and given that Nampt cardiac expression level is decreased in $Lmna^{H222P/H222P}$ mice, providing NAM should neither restore the cardiac NAD$^+$ content nor improve the left-ventricular dysfunction. We treated $Lmna^{H222P/H222P}$ mice with NAM (500 mg/kg every other day) starting at 17-weeks of age, for 9 weeks (Fig. 3A). $Lmna^{H222P/H222P}$ mice treated with NAM did not exhibit changes of their NAD$^+$ content in both liver and heart compared with placebo-treated animals (Fig. 3B). Left ventricular structure and function were assessed by echocardiography after 4 weeks of treatment and at the end of the NAM treatment. Compared with placebo-treated $Lmna^{H222P/H222P}$ mice, NAM-treated $Lmna^{H222P/H222P}$ mice had no significant changes in left ventricular end-systolic and left ventricular end-diastolic diameters as well

Table 1. Echocardiographic parameters for WT and $Lmna^{H222P/H222P}$ mice fed with either NR or chow diet

Genotype	WT	WT	$Lmna^{H222P/H222P}$	$Lmna^{H222P/H222P}$
Treatment	Chow-diet	NR-diet	Chow-diet	NR-diet
n	13	12	11	31
Age, weeks	17	17	17	17
Heart rate, bpm	534.8 ± 35.5	553.9 ± 17.8	531.1 ± 34.8	549.2 ± 31,6
IVSd, mm	0.62 ± 0.01	0.63 ± 0.02	0.59 ± 0.01	0.62 ± 0.01
LVPWd, mm	0.58 ± 0.03	0.60 ± 0.02	0.62 ± 0.02	0.62 ± 0.01
LVDd, mm	3.73 ± 0.11	3.68 ± 0.06	4.07 ± 0.11[#]	3.80 ± 0.06
IVSs, mm	0.98 ± 0.03	1.02 ± 0.02	0.93 ± 0.02	1.00 ± 0.02[*]
LVPWs, mm	0.96 ± 0.04	1.00 ± 0.03	0.95 ± 0.03	0.98 ± 0.02
LVDs, mm	2.25 ± 0.11	2.12 ± 0.04	2.80 ± 0.14[#]	2.42 ± 0.06[**]
FS, %	39.99 ± 1.26	42.91 ± 0.44	31.65 ± 1.82[##]	36.57 ± 0.94[*]
Genotype	WT	WT	$Lmna^{H222P/H222P}$	$Lmna^{H222P/H222P}$
Treatment	Chow-diet	NR-diet	Chow-diet	NR-diet
n	13	12	11	24
Age, weeks	21	21	21	21
Heart rate, bpm	560.1 ± 26.3	570.3 ± 42.13	551.1 ± 34.7	564.2 ± 36.2
IVSd, mm	0.67 ± 0.01	0.68 ± 0.01	0.54 ± 0.02[###]	0.63 ± 0.01[***]
LVPWd, mm	0.69 ± 0.02	0.72 ± 0.02	0.52 ± 0.03[###]	0.61 ± 0.02[**]
LVDd, mm	3.76 ± 0.07	3.73 ± 0.10	4.37 ± 0.15[###]	3.96 ± 0.05[**]
IVSs, mm	1.15 ± 0.02	1.13 ± 0.03	0.77 ± 0.04[###]	1.03 ± 0.02[***]
LVPWs, mm	1.11 ± 0.03	1.13 ± 0.01	0.75 ± 0.03[###]	0.97 ± 0.03[***]
LVDs, mm	2.10 ± 0.04	2.06 ± 0.08	3.42 ± 0.22[###]	2.53 ± 0.07[***]
FS, %	44.42 ± 0.46	45.01 ± 0.87	26.14 ± 2.41[###]	36.20 ± 1.26[**]
Genotype	WT	WT	$Lmna^{H222P/H222P}$	$Lmna^{H222P/H222P}$
Treatment	Chow-diet	NR-diet	Chow-diet	NR-diet
n	13	12	9	31
Age, weeks	26	26	26	26
Heart rate, bpm	537.6 ± 28.9	558.5 ± 26.8	536.2 ± 37.8	555.1 ± 32.7
IVSd, mm	0.64 ± 0.01	0.66 ± 0.01	0.57 ± 0.02[#]	0.63 ± 0.01[*]
LVPWd, mm	0.73 ± 0.02	0.70 ± 0.03	0.48 ± 0.04[###]	0.58 ± 0.02[*]
LVDd, mm	3.97 ± 0.13	3.78 ± 0.08	4.32 ± 0.19	4.18 ± 0.06
IVSs, mm	1.05 ± 0.05	1.05 ± 0.03	0.71 ± 0.04[###]	0.97 ± 0.03[***]
LVPWs, mm	1.06 ± 0.03	1.11 ± 0.04	0.71 ± 0.04[###]	0.94 ± 0.03[***]
LVDs, mm	2.52 ± 0.18	2.23 ± 0.10	3.47 ± 0.23[#]	2.90 ± 0.10[*]
FS, %	37.62 ± 2.49	41.20 ± 1.48	20.63 ± 2.17[###]	30.89 ± 1.57[**]

IVS, inter ventricular septum; LVPW, left ventricular posterior wall; LVD, left ventricular diameter; FS, fractional shortening; s, systole; d, diastole. Values are means ± standard errors of means. [#]P-value ≤ 0.01, [##]P-value ≤ 0.001 and [###]P-value ≤ 0.0001 between chow diet-fed WT mice and chow diet-fed $Lmna^{H222P/H222P}$ mice. [*]P-value ≤ 0.01, [**]P-value ≤ 0.001 and [***]P-value ≤ 0.0001 between NR die-fed $Lmna^{H222P/H222P}$ mice and chow diet-fed $Lmna^{H222P/H222P}$ mice.

as fractional shortening (Fig. 3C and D, Table 2). NAM-treated $Lmna^{H222P/H222P}$ mice had no changed expression of cardiac *Myh7*, *Nppa* and *Col1a2* (Fig. 3E). Thus, our data showed that treating $Lmna^{H222P/H222P}$ mice with NAM is not efficient to restore the cardiac NAD$^+$ content and the cardiac left ventricular function.

Decreased cardiac NAD$^+$ content alters global PARylation

We then asked the consequences of decreased cardiac NAD$^+$ on sirtuin 1 (SIRT1) and Poly(ADP-ribose) polymerase 1 (PARP-1) activities. The sirtuins are protein deacetylases, which play roles on mitochondria metabolism (7,24). The NAD$^+$ level has been shown to activate SIRT1, which regulates mitochondria biogenesis through the deacetylation of target proteins. We showed that the level of SIRT1 mRNA (Fig. 4A) and protein (Fig. 4B) expressions were not altered in hearts from $Lmna^{H222P/H222P}$ mice compared with WT mice. The levels of acetylated FOXO1

(Fig. 4C), P65 (Fig. 4D) and p53 (Fig. 4E), known targets of SIRT1 (25–27), were unchanged in hearts from $Lmna^{H222P/H222P}$ mice compared with WT mice. Thus, our data suggested that the decreased cardiac NAD$^+$ content is not altering SIRT1 activity in *LMNA* cardiomyopathy.

PARP enzymes bind and cleave NAD$^+$ to produce NAM and ADP-ribose, and couple one or more ADP-ribose units to promote PARylation of acceptor proteins (28). The level of PARylation detected by poly(ADP-ribose) (PAR) monoclonal antibody was decreased in hearts from $Lmna^{H222P/H222P}$ mice compared with WT mice (Fig. 5A). Feeding $Lmna^{H222P/H222P}$ mice with NR led to a marked increase of cardiac PARylation (Fig. 5A). We next showed that mRNA (Fig. 5B) and protein (Fig. 5C) levels of cardiac PARP-1, the most abundant isoform of the PARP enzyme family, were lowered in $Lmna^{H222P/H222P}$ mice compared with WT mice and increased after NR feeding. We performed immunoprecipitation using extracts of hearts from $Lmna^{H222P/H222P}$ mice and WT mice and antibody against poly(ADP-ribose). We found that the
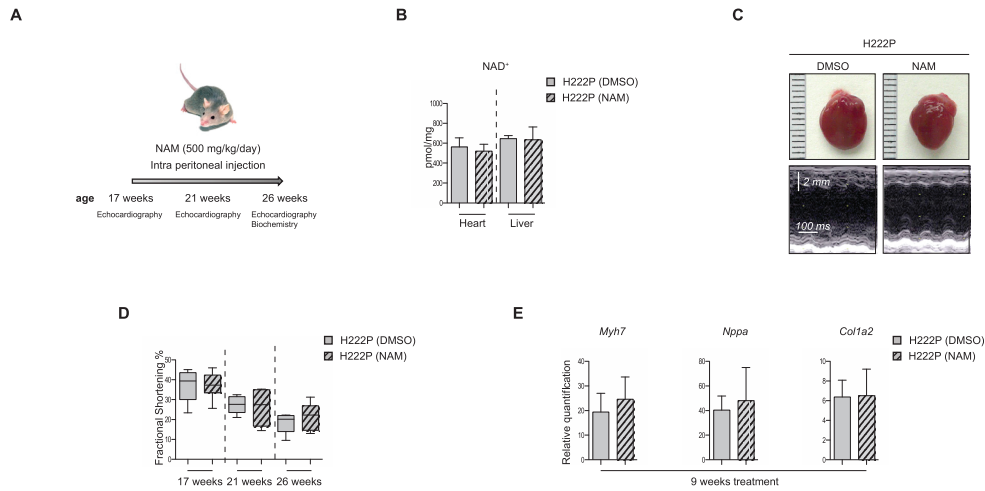
Figure 3. NAM supplementation does not improve cardiac function in *Lmna*[H222P/H222P] mice (**A**) Schematic representation of the treatment protocol of *Lmna*[H222P/H222P] mice with NAM. (**B**) Quantification of NAD+ content (pmol/mg tissue) in heart and liver from placebo-treated *Lmna*[H222P/H222P] (n = 6) mice and NAM-treated *Lmna*[H222P/H222P] (n = 7) mice at 26 weeks. Bars indicate means ± standard errors of means. (**C**) Gross histological examination of heart from placebo-treated and NAM-treated *Lmna*[H222P/H222P] (n = 7) mice at 26 weeks of age. (**D**) Box-and-whisker plots showing median fractional shortening (FS) in 17-, 21- and 26-weeks-old placebo-treated or NAM-treated *Lmna*[H222P/H222P] mice. Values are shown as 25th to 75th percentiles of the ranked set of data values. The line in the middle is plotted as the median. Whiskers (Tukey method) extend down to the minimum value and up to the maximum value. (**E**) Expression of *Myh7*, *Nppa* and *Col1a2* genes by qPCR from cDNAs of heart from placebo or NAM-treated *Lmna*[H222P/H222P] (n = 5) mice.

Table 2. Echocardiographic parameters for male *Lmna*[H222P/H222P] mice treated or not with NAM at 17, 21 and 26 weeks of age

Genotype	*Lmna*[H222P/H222P]	*Lmna*[H222P/H222P]	*Lmna*[H222P/H222P]	*Lmna*[H222P/H222P]	*Lmna*[H222P/H222P]	*Lmna*[H222P/H222P]
Treatment	Placebo	NAM	Placebo	NAM	Placebo	NAM
n	6	7	5	6	5	5
Age, weeks	17	17	21	21	26	26
Heart rate, bpm	534.0 ± 35.52	553.9 ± 17.82	531.1 ± 34.84	549.2 ± 31.65	560.1 ± 26.31	570.3 ± 42.13
IVSd, mm	0.65 ± 0.03	0.71 ± 0.03	0.64 ± 0.02	0.68 ± 0.02	0.56 ± 0.02	0.64 ± 0.02
LVPWd, mm	0.60 ± 0.03	0.63 ± 0.02	0.56 ± 0.05	0.60 ± 0.03	0.58 ± 0.04	0.46 ± 0.02
LVDd, mm	4.10 ± 0.21	3.94 ± 0.23	4.42 ± 0.15	4.45 ± 0.27	4.76 ± 0.13	4.68 ± 0.22
IVSs, mm	1.10 ± 0.05	1.09 ± 0.05	0.92 ± 0.04	0.95 ± 0.04	0.86 ± 0.07	0.92 ± 0.07
LVPWs, mm	1.07 ± 0.03	1.07 ± 0.04	0.88 ± 0.05	0.78 ± 0.04	0.70 ± 0.05	0.72 ± 0.05
LVDs, mm	2.60 ± 0.27	2.50 ± 0.24	3.22 ± 0.18	3.33 ± 0.36	3.92 ± 0.19	3.64 ± 0.28
FS, %	37.08 ± 3.30	37.40 ± 2.55	27.49 ± 1.97	26.18 ± 3.55	18.34 ± 2.33	21.55 ± 2.76

IVS, inter ventricular septum; LVPW, left ventricular posterior wall; LVD, left ventricular diameter; FS, fractional shortening; s: systole; d: diastole. Values are means ± standard errors of means.

PARylation of cardiac PARP-1 was lowered in *Lmna*[H222P/H222P] mice compared with WT mice (Fig. 5D). Therefore, these results showed that the drop in NAD+ cardiac content in *Lmna*[H222P/H222P] mice was altering PARP-1 activity.

Discussion

Altered NAD+ metabolism through the salvage pathway has been described in muscular dystrophies (25,29–31) and aging process (32–37). We expand the current knowledge by showing that altered NAD+ salvage causes heart failure and inherited cardiomyopathy. We demonstrate that oral supplementation with NR, a vitamin B3 form and NAD+ precursor, efficiently prevented development and progression of *LMNA* cardiomyopathy in mice. We show that NR supplementation significantly delayed disease progression even in mice that already manifested the disease, which is the time frame when medicated treatment would typically be started for patients. These results are remarkable, as they underline the utmost importance of specific vitamin co-factors, as modifiers of metabolism in cardiac

disease, and emphasize the role of nutritional signaling in the pathogenesis of *LMNA* cardiomyopathy. The results presented in this study are in line with previous work showing that exogenous NAD+ content blocks cardiac hypertrophy, (9,11). A recent study demonstrated that NR treatment transiently rescued the cardiomyopathy in iron deficiency mouse model (38). Similarly, increasing the NAD+ content using precursors of NAD+ has been proven efficient to rescue hallmark of mitochondrial myopathy both in mouse (29) and human (39), as well as in aging (36,40). How decreased NAD+ results in cardiac tissue injury in *LMNA* cardiomyopathy is yet to be fully elucidated and this would need further investigation.

We showed that PARylation is altered in *LMNA* cardiomyopathy, ensuing decreased cardiac NAD+. PARP enzymes bind and cleave NAD+ to nicotinamide and charged PAR polymers on a large set of target proteins (41). Given its DNA-binding zinc fingers (41,42) PARP-1 can be activated through DNA breaks (43) and irregular DNA structures (44), and thus cleaves NAD+ generating NAM and ADP-ribose. In the attempt to repair DNA lesions, PARP-1 activation takes place by adding ADP-ribose units to form
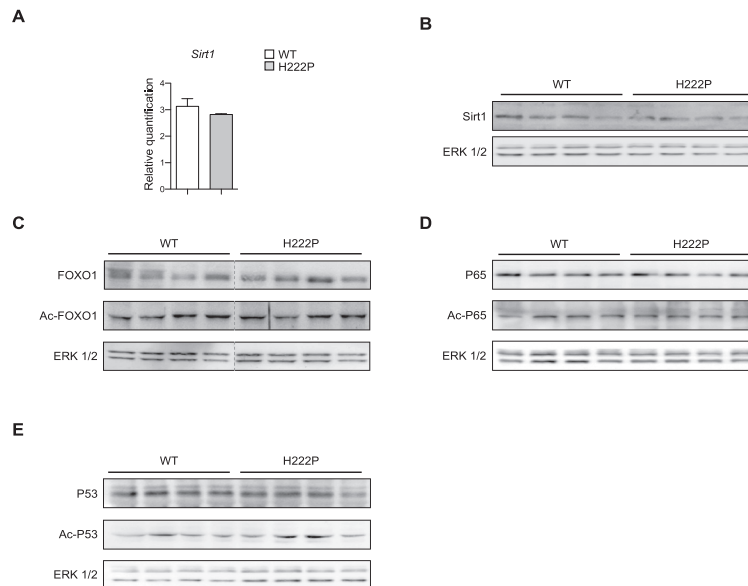
Figure 4. NAD$^+$ depletion does not alter SIRT1-dependent lysine acetylation in *LMNA* cardiomyopathy. (**A**) Expression of *Sirt1* mRNA in hearts from a 26-week-old male WT (n = 4) and *Lmna*$^{H222P/H222P}$ (n = 4) mice. Data are represented as means ± standard errors of means. (**B**) Immunoblots showing Sirt1 protein level expression in a 26-week-old male WT and *Lmna*$^{H222P/H222P}$ mice. (**C**) Immunoblots showing acetylated-FOXO1 and total FOXO1 protein level expression in a 26-week-old male WT and *Lmna*$^{H222P/H222P}$ mice. (**D**) Immunoblots showing acetylated-P65 and total P65 protein level expression in a 26-week-old male WT and *Lmna*$^{H222P/H222P}$ mice. (**E**) Immunoblots showing acetylated-P53 and total P53 protein level expression in a 26-week-old male WT and *Lmna*$^{H222P/H222P}$ mice.

chains of PAR covalently attached to acceptor proteins, among which PARP-1, to facilitate the DNA repair machinery (45,46). It would be of interest to further investigate that the inhibition of PARP-1, and its PARylation, by the decreased cardiac NAD$^+$ content in *Lmna*$^{H222P/H222P}$ mice, could fail to trigger adaptive mechanisms, such as DNA repair, in the development of *LMNA* cardiomyopathy.

In conclusion, our experiments demonstrate a novel contributory metabolic mechanism for *LMNA* cardiomyopathy triggered by altered NAD$^+$ salvage pathway. Moreover, we have shown that modulation of cardiac NAD$^+$ content using NR is a straightforward therapeutic strategy. Given that vitamin B3 supplement is potentially translatable into therapy, our work supports more studies on human to begin to evaluate the therapeutic benefits of increasing NAD$^+$ and assess the benefit of such therapy on *LMNA* cardiomyopathy. Accordingly, recent work described that normalization of NAD$^+$ content could be used as a pharmacologic strategy in failing heart (11,47) and a clinical trial to assess the benefit of NR in systolic heart failure is on-going (NCT03423342). This novel therapy would need to be associated with reduced risks, particularly as the treatment may be needed for years. The translation from bench-to-bedside could be seen in years to come since precursors of NAD$^+$ [e.g. Acipimox (48,49), Nicobion, Nicorandil] have already been used in therapeutics (50–53). Recently, it has been shown that a single dose of NR resulted in significant increases in NAD$^+$ in healthy human volunteers (23). Overall, our work provides adequate grounds for a therapeutic approach based on NR for patients with *LMNA* cardiomyopathy.

Experimental Procedures

Human heart tissue

Explanted hearts from human subjects with *LMNA* cardiomyopathy were obtained from Myobank-AFM from the Institut de Myologie (Paris, France). The subjects were a 23-year-old man carrying the *LMNA* c.781-783delAAG, p.Lys261del mutation and a 47-year-old woman carrying the *LMNA* c.178C > G, p.Arg60Gly mutation. Control human heart samples were obtained from the National Disease Research Interchange (Philadelphia, PA, USA) from a 15-year-old girl who died of overdose and a 57-year-old man who died of cerebrovascular accident. Tissue samples received from either autopsy or transplanted consent donors were not obtained specifically for this study and provided by Myobank-AFM or the National Disease Research Interchange without patient identifiers.

Animals

All animal experiments were approved by the French Ministry of Health at the Center for Research in Myology for the Care and Use of Experimental Animals (approval number #6455). The animal experiments were performed according to the guidelines from Directive 2010/63/EU of the European Parliament on the protection of animals used for scientific purposes. *Lmna*$^{H222P/H222P}$ mice were fed chow and housed in a disease-free barrier facility with 12 h light/12 h dark cycles. Chow supplemented with 0.25% NR (400 mg/kg) (Chromadex), as previously reported (27), was formulated by Scientific Animal Food and Engineering. For post-symptomatic treatment, NR was delivered to *Lmna*$^{H222P/H222P}$ mice at a dose of 400/kg per day orally by gavage. NR was formulated in water and water was used as placebo. NAM was delivered to a concentration of 500 mg/kg every other day by intraperitoneal injection using a 27 G 5/8 syringe. NAM was formulated in physiologic serum and physiologic serum was used as placebo. For survival analysis, *Lmna*$^{H222P/H222P}$ mice were fed chow supplemented with 0.25% NR when they were 17 weeks of age and continued until they suffered from significant distress or died.

Echocardiography

Lmna$^{H222P/H222P}$ and WT mice were anesthetized with 0.75% isoflurane in O$_2$ and placed on a heating pad (25°C). Echocardiography
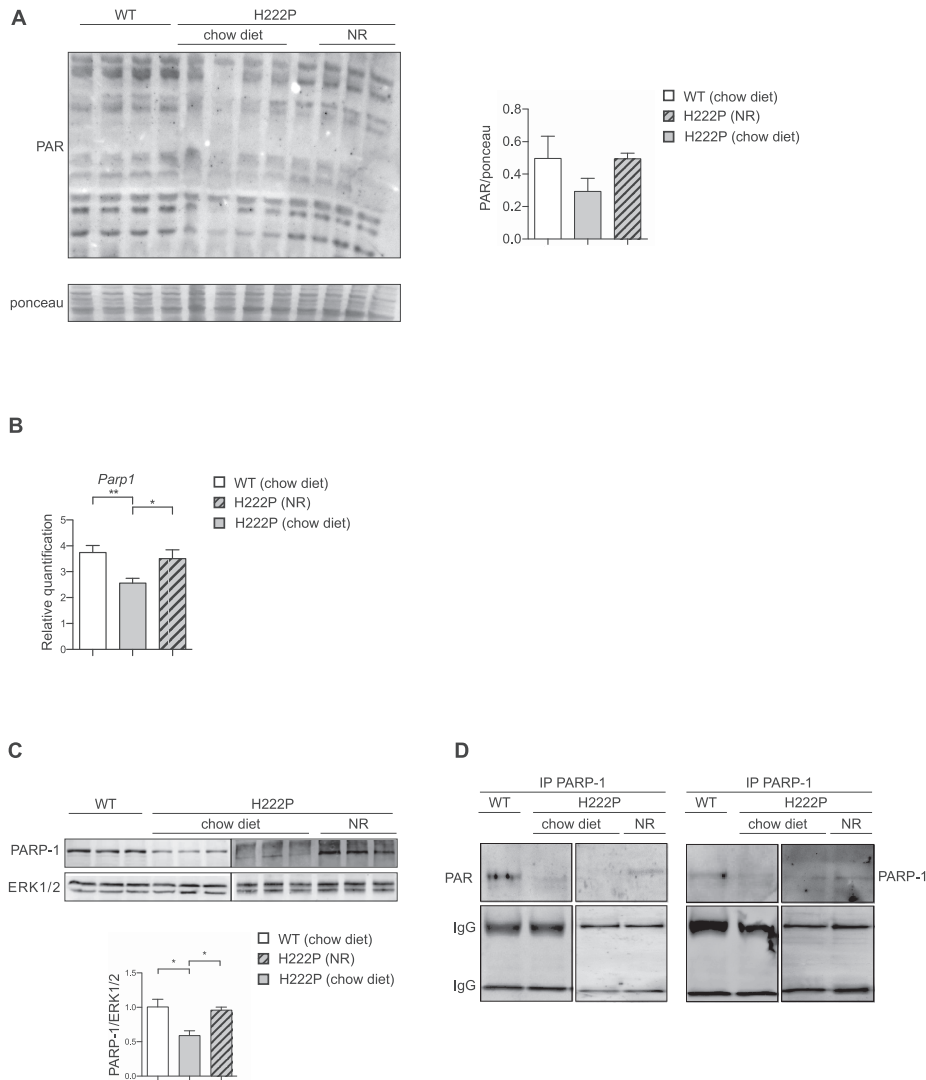
Figure 5. NAD$^+$ depletion causes decrease in global PARylation. (**A**) Immunoblots showing total PARylated protein level expression (PAR antibody) in hearts from a 26-week-old WT (n = 3) and from a 26-week-old chow diet-fed *Lmna*$^{H222P/H222P}$ (H222P) (n = 6) mice and in NR-fed *Lmna*$^{H222P/H222P}$ (n = 3) mice. ERK1/2 was shown as loading control. The bar graphs represent PARylated protein relative expression (mean ± standard error of means) (relative to ponceau). (**B**) Expression of *Parp1* gene by qPCR from cDNAs of heart from WT (n = 5), chow diet-fed (n = 5) or NR-fed *Lmna*$^{H222P/H222P}$ (n = 5). *P-value ≤ 0.01, **P-value ≤ 0.001. (**C**) Immunoblots showing PARP-1 protein level in hearts from a 26-week-old WT (n = 3) and from a 26-week-old chow diet-fed *Lmna*$^{H222P/H222P}$ (H222P) (n = 6) mice and in NR-fed *Lmna*$^{H222P/H222P}$ (n = 3) mice. The bar graphs represent protein relative expression (means ± standard errors of means) of PARP-1 (relative to ERK1/2). *P-value ≤ 0.01. (**D**) Representative immunoprecipitation showing PARylated PARP-1 level in hearts from a 26-week-old WT, *Lmna*$^{H222P/H222P}$ and NR fed *Lmna*$^{H222P/H222P}$ mice. Immunoprecipitation showing PARP-1 level in hearts from a 26-week-old WT *Lmna*$^{H222P/H222P}$ and NR-fed *Lmna*$^{H222P/H222P}$ mice was shown as control.

was performed using an ACUSON 128XP/10 ultrasound with an 11 MHz transducer applied to the chest wall. Cardiac ventricular dimensions and fractional shortening were measured in 2D mode and M-mode 3 times for the number of animals indicated. A 'blinded' echocardiographer, unaware of the genotype and the treatment, performed the examinations.

qPCR analysis

Total RNA was extracted using the RNeasy Mini kit (Qiagen). cDNA was synthesized using the SuperScript III synthesis system according to the manufacturer's instructions (Invitrogen). Real-time qPCR reactions were performed with SYBR Green I Master mix (Roche) using with the LightCycler 480 (Roche). Relative levels of mRNA expression calculated using the $\Delta\Delta C_T$ method were normalized by comparison to housekeeping mRNA (54). The listing of primers can be found in Supplementary Material Table S3.

Immunoblotting

Mouse heart tissues were homogenized in sample extraction buffer (Cell Signaling) completed with deacetylation inhibitors cocktail (Santa Cruz Biotechnology) then separated by 10% SDS-polyacrylamide gel electrophoresis, transferred to nitrocellulose membranes and blotted with primary antibodies (Supplementary Material, Table S4). Secondary antibodies were horseradish peroxidate-conjugate (Jackson ImmunoResearch). Recognized proteins were visualized by enhanced chemiluminescence.

NAD⁺ concentration quantification.

Fresh mouse tissues were homogenized and processed according to previous report (55). The concentration of cardiac and liver NAD⁺ was determined using a spectrophotometric assay as described previously (56). Absorption measurements were carried out in 96-well plates by spectrophotometry (Tecan).

Statistics.

Values for real-time q-PCR, immunoblots and NAD⁺ content were compared using an unpaired Student's t-test. Comparisons of echocardiographic parameters between groups of $Lmna^{H222P/H222P}$ mice (treated and untreated) were performed using a Welch t-test; to validate these results, a non-parametric test (Mann–Whitney) was performed and concordance checked. Statistical analyses were performed using Prism 6.0 software (Graphpad).

Supplementary Material

Supplementary Material is available at *HMG* online.

Acknowledgements

Funding

References

1. Bogan, K.L. and Brenner, C. (2008) Nicotinic acid, nicotinamide, and nicotinamide riboside: a molecular evaluation of NAD+ precursor vitamins in human nutrition. *Annu. Rev. Nutr.*, **28**, 115–130.
2. Chi, Y. and Sauve, A.A. (2013) Nicotinamide riboside, a trace nutrient in foods, is a vitamin B3 with effects on energy metabolism and neuroprotection. *Curr. Opin. Clin. Nutr. Metab. Care*, **16**, 657–661.
3. Houtkooper, R.H., Cantó, C., Wanders, R.J. and Auwerx, J. (2010) The secret life of NAD+: an old metabolite controlling new metabolic signaling pathways. *Endocr. Rev.*, **31**, 194–223.
4. Bieganowski, P. and Brenner, C. (2004) Discoveries of nicotinamide riboside as a nutrient and conserved NRK genes establish a Preiss-Handler independent route to NAD+ in fungi and humans. *Cell*, **117**, 495–502.
5. Ratajczak, J., Joffraud, M., Trammell, S.A.J., Ras, R., Canela, N., Boutant, M., Kulkarni, S.S., Rodrigues, M., Redpath, P., Migaud, M.E. *et al.* (2016) NRK1 controls nicotinamide mononucleotide and nicotinamide riboside metabolism in mammalian cells. *Nat. Commun.*, **7**, 13103.
6. Garten, A., Schuster, S., Penke, M., Gorski, T., Giorgis, T. de and Kiess, W. (2015) Physiological and pathophysiological roles of NAMPT and NAD metabolism. *Nat. Rev. Endocrinol.*, **11**, 535–546.
7. Stein, L.R. and Imai, S. (2012) The dynamic regulation of NAD metabolism in mitochondria. *Trends Endocrinol. Metab.*, **23**, 420–428.
8. Hsu, C.-P., Oka, S., Shao, D., Hariharan, N. and Sadoshima, J. (2009) Nicotinamide phosphoribosyltransferase regulates cell survival through NAD+ synthesis in cardiac myocytes. *Circ. Res.*, **105**, 481–491.
9. Pillai, V.B., Sundaresan, N.R., Kim, G., Gupta, M., Rajamohan, S.B., Pillai, J.B., Samant, S., Ravindra, P.V., Isbatan, A. and Gupta, M.P. (2010) Exogenous NAD blocks cardiac hypertrophic response via activation of the SIRT3-LKB1-AMP-activated kinase pathway. *J. Biol. Chem.*, **285**, 3133–3144.
10. Dou, Q., Peng, Y., Zhou, B., Zhang, K., Lin, J., Dai, X., Zhang, L. and Rao, L. (2015) Association of nicotinamide phosphoribosyltransferase (NAMPT) gene polymorphisms and of serum NAMPT levels with dilated cardiomyopathy in a Chinese population. *Int. J. Mol. Sci.*, **16**, 22299–22318.
11. Diguet, N., Trammell, S.A.J., Tannous, C., Deloux, R., Piquereau, J., Mougenot, N., Gouge, A., Gressette, M., Manoury, B., Blanc, J., *et al.* (2017) Nicotinamide riboside preserves cardiac function in a mouse model of dilated cardiomyopathy. *Circulation*, 10.1161/CIRCULATIONAHA.116.026099.
12. Martin, A.S., Abraham, D.M., Hershberger, K.A., Bhatt, D.P., Mao, L., Cui, H., Liu, J., Liu, X., Muehlbauer, M.J., Grimsrud, P.A. *et al.* Nicotinamide mononucleotide requires SIRT3 to improve cardiac function and bioenergetics in a Friedreich's ataxia cardiomyopathy model. *JCI Insight*, **2**, pii:93885.
13. Kuno, A., Hori, Y.S., Hosoda, R., Tanno, M., Miura, T., Shimamoto, K. and Horio, Y. (2013) Resveratrol improves cardiomyopathy in dystrophin-deficient mice through SIRT1 protein-mediated modulation of p300 protein. *J. Biol. Chem.*, **288**, 5963–5972.
14. Elliott, P., Andersson, B., Arbustini, E., Bilinska, Z., Cecchi, F., Charron, P., Dubourg, O., Kühl, U., Maisch, B., McKenna, W.J. *et al.* (2008) Classification of the cardiomyopathies: a position statement from the european society of cardiology working group on myocardial and pericardial diseases. *Eur. Heart J.*, **29**, 270–276.
15. Lin, F. and Worman, H.J. (1993) Structural organization of the human gene encoding nuclear lamin A and nuclear lamin C. *J. Biol. Chem.*, **268**, 16321–16326.
16. Fatkin, D., MacRae, C., Sasaki, T., Wolff, M.R., Porcu, M., Frenneaux, M., Atherton, J., Vidaillet, H.J.J., Spudich, S., De Girolami, U. *et al.* (1999) Missense mutations in the rod domain of the lamin A/C gene as causes of dilated cardiomyopathy and conduction-system disease. *N. Engl. J. Med.*, **341**, 1715–1724.
17. Bonne, G., Barletta, M.R.D., Varnous, S., Bécane, H.-M., Hammouda, E.-H., Merlini, L., Muntoni, F., Greenberg, C.R., Gary, F., Urtizberea, J.-A. *et al.* (1999) Mutations in the gene encoding lamin A/C cause autosomal dominant Emery-Dreifuss muscular dystrophy. *Nat. Genet.*, **21**, 285–288.
18. Arimura, T., Helbling-Leclerc, A., Massart, C., Varnous, S., Niel, F., Lacène, E., Fromes, Y., Toussaint, M., Mura, A.-M., Keller, D.I. *et al.* (2005) Mouse model carrying H222P-Lmna mutation develops muscular dystrophy and dilated cardiomyopathy similar to human striated muscle laminopathies. *Hum. Mol. Genet.*, **14**, 155–169.
19. Bonne, G., Mercuri, E., Muchir, A., Urtizberea, A., Bécane, H.M., Recan, D., Merlini, L., Wehnert, M., Boor, R., Reuner, U. *et al.* (2000) Clinical and molecular genetic spectrum of autosomal dominant Emery-Dreifuss muscular dystrophy due to mutations of the lamin A/C gene. *Ann. Neurol.*, **48**, 170–180.
20. Cattin, M.-E., Bertrand, A.T., Schlossarek, S., Le Bihan, M.-C., Skov Jensen, S., Neuber, C., Crocini, C., Maron, S., Lainé, J.,

Mougenot, N. *et al.* (2013) Heterozygous LmnadelK32 mice develop dilated cardiomyopathy through a combined pathomechanism of haploinsufficiency and peptide toxicity. *Hum. Mol. Genet.*, **22**, 3152–3164.

21. Akbay, E.A., Moslehi, J., Christensen, C.L., Saha, S., Tchaicha, J.H., Ramkissoon, S.H., Stewart, K.M., Carretero, J., Kikuchi, E., Zhang, H. *et al.* (2014) D-2-hydroxyglutarate produced by mutant IDH2 causes cardiomyopathy and neurodegeneration in mice. *Genes Dev.*, **28**, 479–490.

22. Wang, T., Lang, G.D., Moreno-Vinasco, L., Huang, Y., Goonewardena, S.N., Peng, Y., Svensson, E.C., Natarajan, V., Lang, R.M., Linares, J.D. *et al.* (2012) Particulate matter induces cardiac arrhythmias via dysregulation of carotid body sensitivity and cardiac sodium channels. *Am. J. Respir. Cell Mol. Biol.*, **46**, 524–531.

23. Trammell, S.A.J., Schmidt, M.S., Weidemann, B.J., Redpath, P., Jaksch, F., Dellinger, R.W., Li, Z., Abel, E.D., Migaud, M.E. and Brenner, C. (2016) Nicotinamide riboside is uniquely and orally bioavailable in mice and humans. *Nat. Commun.*, **7**, 12948.

24. Verdin, E. (2015) NAD+ in aging, metabolism, and neurodegeneration. *Science*, **350**, 1208–1213.

25. Ryu, D., Zhang, H., Ropelle, E.R., Sorrentino, V., Mázala, D.A.G., Mouchiroud, L., Marshall, P.L., Campbell, M.D., Ali, A.S., Knowels, G.M. *et al.* (2016) NAD+ repletion improves muscle function in muscular dystrophy and counters global PARylation. *Sci. Transl. Med.*, **8**, 361ra139.

26. Yang, H., Zhang, W., Pan, H., Feldser, H.G., Lainez, E., Miller, C., Leung, S., Zhong, Z., Zhao, H., Sweitzer, S. *et al.* (2012) SIRT1 activators suppress inflammatory responses through promotion of p65 deacetylation and inhibition of NF-κB activity. *PLoS ONE*, **7**, e46364.

27. Vaziri, H., Dessain, S.K., Ng Eaton, E., Imai, S.I., Frye, R.A., Pandita, T.K., Guarente, L. and Weinberg, R.A. (2001) hSIR2(SIRT1) functions as an NAD-dependent p53 deacetylase. *Cell*, **107**, 149–159.

28. Bai, P. (2015) Biology of poly(ADP-Ribose) polymerases: the factotums of cell maintenance. *Mol. Cell*, **58**, 947–958.

29. Khan, N.A., Auranen, M., Paetau, I., Pirinen, E., Euro, L., Forsström, S., Pasila, L., Velagapudi, V., Carroll, C.J., Auwerx, J. *et al.* (2014) Effective treatment of mitochondrial myopathy by nicotinamide riboside, a vitamin B3. *EMBO Mol. Med.*, **6**, 721–731.

30. Hori, Y.S., Kuno, A., Hosoda, R., Tanno, M., Miura, T., Shimamoto, K. and Horio, Y. (2011) Resveratrol ameliorates muscular pathology in the dystrophic mdx mouse, a model for duchenne muscular dystrophy. *J. Pharmacol. Exp. Ther.*, **338**, 784–794.

31. Goody, M.F., Kelly, M.W., Reynolds, C.J., Khalil, A., Crawford, B.D. and Henry, C.A. (2012) NAD+ biosynthesis ameliorates a zebrafish model of muscular dystrophy. *PLOS Biol.*, **10**, e1001409.

32. Balan, V., Miller, G.S., Kaplun, L., Balan, K., Chong, Z.-Z., Li, F., Kaplun, A., VanBerkum, M.F.A., Arking, R., Freeman, D.C. *et al.* (2008) Life span extension and neuronal cell protection by Drosophila nicotinamidase. *J. Biol. Chem.*, **283**, 27810–27819.

33. Belenky, P., Racette, F.G., Bogan, K.L., McClure, J.M., Smith, J.S. and Brenner, C. (2007) Nicotinamide riboside promotes Sir2 silencing and extends lifespan via Nrk and Urh1/Pnp1/Meu1 pathways to NAD+. *Cell*, **129**, 473–484.

34. Massudi, H., Grant, R., Braidy, N., Guest, J., Farnsworth, B. and Guillemin, G.J. (2012) Age-associated changes in oxidative stress and NAD+ metabolism in human tissue. *PLoS ONE*, **7**, e42357.

35. Mouchiroud, L., Houtkooper, R.H., Moullan, N., Katsyuba, E., Ryu, D., Cantó, C., Mottis, A., Jo, Y.-S., Viswanathan, M., Schoonjans, K. *et al.* (2013) The NAD(+)/sirtuin pathway modulates longevity through activation of mitochondrial UPR and FOXO signaling. *Cell*, **154**, 430–441.

36. Zhang, H., Ryu, D., Wu, Y., Gariani, K., Wang, X., Luan, P., D'Amico, D., Ropelle, E.R., Lutolf, M.P., Aebersold, R. *et al.* (2016) NAD+ repletion improves mitochondrial and stem cell function and enhances life span in mice. *Science*, **352**, 1436–1443.

37. Zhu, X.-H., Lu, M., Lee, B.-Y., Ugurbil, K. and Chen, W. (2015) In vivo NAD assay reveals the intracellular NAD contents and redox state in healthy human brain and their age dependences. *Proc. Natl. Acad. Sci. U. S. A.*, **112**, 2876–2881.

38. Xu, W., Barrientos, T., Mao, L., Rockman, H.A., Sauve, A.A. and Andrews, N.C. (2015) Lethal cardiomyopathy in mice lacking transferrin receptor in the heart. *Cell Rep.*, **13**, 533–545.

39. Weijer, T. van de, Phielix, E., Bilet, L., Williams, E.G., Ropelle, E.R., Bierwagen, A., Livingstone, R., Nowotny, P., Sparks, L.M., Paglialunga, S., *et al.* (2015) Evidence for a direct effect of the NAD+ precursor acipimox on muscle mitochondrial function in humans. *Diabetes*, **64**, 1193–1201.

40. Rajman, L., Chwalek, K. and Sinclair, D.A. (2018) Therapeutic Potential of NAD-Boosting Molecules: The In Vivo Evidence. *Cell Metab.*, **27**, 529–547.

41. Alvarez-Gonzalez, R. and Mendoza-Alvarez, H. (1995) Dissection of ADP-ribose polymer synthesis into individual steps of initiation, elongation, and branching. *Biochimie*, **77**, 403–407.

42. Langelier, M.-F., Planck, J.L., Roy, S. and Pascal, J.M. (2012) Structural basis for DNA-dependent poly(ADP-ribosyl)ation by human PARP-1. *Science*, **336**, 728–732.

43. Benjamin, R.C. and Gill, D.M. (1980) Poly(ADP-ribose) synthesis in vitro programmed by damaged DNA. A comparison of DNA molecules containing different types of strand breaks. *J. Biol. Chem*, **255**, 10502–10508.

44. Kun, E., Kirsten, E. and Ordahl, C.P. (2002) Coenzymatic activity of randomly broken or intact double-stranded DNAs in auto and histone H1 trans-poly(ADP-ribosylation), catalyzed by poly(ADP-ribose) polymerase (PARP I). *J. Biol. Chem.*, **277**, 39066–39069.

45. Javle, M. and Curtin, N.J. (2011) The role of PARP in DNA repair and its therapeutic exploitation. *Br. J. Cancer*, **105**, 1114–1122.

46. De Vos, M., Schreiber, V. and Dantzer, F. (2012) The diverse roles and clinical relevance of PARPs in DNA damage repair: current state of the art. *Biochem. Pharmacol.*, **84**, 137–146.

47. Lee, C.F., Chavez, J.D., Garcia-Menendez, L., Choi, Y., Roe, N.D., Chiao, Y.A., Edgar, J.S., Goo, Y.A., Goodlett, D.R., Bruce, J.E. *et al.* (2016) Normalization of NAD+ redox balance as a therapy for heart failure. *Circulation*, **134**, 883–894.

48. Fuccella, L.M., Goldaniga, G., Lovisolo, P., Maggi, E., Musatti, L., Mandelli, V. and Sirtori, C.R. (1980) Inhibition of lipolysis by nicotinic acid and by acipimox. *Clin. Pharmacol. Ther.*, **28**, 790–795.

49. Musatti, L., Maggi, E., Moro, E., Valzelli, G. and Tamassia, V. (1981) Bioavailability and pharmacokinetics in man of acipimox, a new antilipolytic and hypolipemic agent. *J. Int. Med. Res.*, **9**, 381–386.

50. Ball, M.J., Vella, M., Rechlass, J.P., Jones, D.B., Stirling, C., Mann, J.I. and Galton, D. (1986) Acipimox in the treatment of patients with hyperlipidaemia: a double blind trial. *Eur. J. Clin. Pharmacol.*, **31**, 201–204.

51. Chen, A.C., Martin, A.J., Choy, B., Fernández-Peñas, P., Dalziell, R.A., McKenzie, C.A., Scolyer, R.A., Dhillon, H.M., Vardy, J.L., Kricker, A. *et al.* (2015) A phase 3 randomized trial of nicotinamide for skin-cancer chemoprevention. *N. Engl. J. Med.*, **373**, 1618–1626.

52. Ishii, H., Ichimiya, S., Kanashiro, M., Amano, T., Imai, K., Murohara, T. and Matsubara, T. (2005) Impact of a single intravenous administration of nicorandil before reperfusion in patients with ST-segment-elevation myocardial infarction. *Circulation*, **112**, 1284–1288.

53. IONA Study Group (2002) Effect of nicorandil on coronary events in patients with stable angina: the impact of nicorandil in angina (IONA) randomised trial. *Lancet Lond. Engl.*, **359**, 1269–1275.

54. Pfaffl, M.W. (2001) A new mathematical model for relative quantification in real-time RT–PCR. *Nucleic Acids Res.*, **29**, e45–e45.

55. Sander, B.J., Oelshlegel, F.J. and Brewer, G.J. (1976) Quantitative analysis of pyridine nucleotides in red blood cells: a single-step extraction procedure. *Anal. Biochem.*, **71**, 29–36.

56. Bernofsky, C. and Swan, M. (1973) An improved cycling assay for nicotinamide adenine dinucleotide. *Anal. Biochem.*, **53**, 452–458.